Preprints (www.preprints.org) | NOT PEER-REVIEWED | Posted: 24 January 2019 doi:10.20944/preprints201901.0244.v1

Peer-reviewed version available at Coatings 2019, 9, 79; doi:10.3390/coatings9020079

Article

Coatings Thickness Determination Using X-ray Fluorescence Spectroscopy: Monte Carlo Simulations as an Alternative to the Use of Standards

Walter Giurlani [1,*], E. Berretti [2], Massimo Innocenti [1,2] and Alessandro Lavacchi [2,*]

[1] Dipartimento di Chimica, Università degli Studi di Firenze, via della Lastruccia 3, 50019 Sesto Fiorentino (FI), Italy; m.innocenti@unifi.it

[2] Consiglio Nazionale delle Ricerche—Istituto di Chimica dei Composti OrganoMetallici (CNR-ICCOM), via Madonna del Piano 10, 50019 Sesto Fiorentino (FI), Italy

* Correspondence: walter.giurlani@unifi.it (W.G.); alessandro.lavacchi@iccom.cnr.it (A.L.); Tel.: +39-055-457-3102 (W.G.); +39-055-522-5250 (A.L.)

Abstract: X-ray fluorescence is largely employed in the measurement of the thickness of coatings. Despite of its diffusion, the task is not straightforward because of the complex physics involved that results in high dependence on matrix effects. Thickness quantification is in practice accomplished using the Fundamental Parameters approach, adjusted with empirical measurements of standards with known composition and thickness. This approach has two major drawbacks: i) there are no standards for any possible coating and coating architecture and ii) even relying on standards, the quantification of unknown samples requires the precise knowledge of the matrix nature (e.g. in case of multilayer coatings the thickness and the composition of each underlayer). In this work, we describe a semiquantitative approach to coatings thickness measurement based on the construction of calibration curves through simulated XRF spectra built with Monte Carlo simulations. Simulations have been performed with the freeware software XMI-MSIM. We have assessed the accuracy of the methods by comparing the results with those obtained by i) XRF thickness determination with standards and ii) FIB-SEM cross-sectioning. Then we evaluated which parameters are critical in this kind of indirect thickness measurements.

Keywords: XRF; X-ray fluorescence; thickness determination; thin film; simulation; XMI-MSIM; electrodeposition; Monte Carlo; galvanic industry; electroplating

1. Introduction

Thickness is a crucial parameter in coatings technology and affects much materials functionality. Thickness determination of metallic and ceramic coatings is often performed by X-ray Fluorescence (XRF), a widespread non-destructive technique largely applied in industry as a tool for Quality Assurance (QA) and Materials Science R&D [1–5]. Deriving coatings thickness from the X-ray spectrum requires an experimental calibration curve that employs standards; however, due to the large dependence of the X-ray spectrum on the nature of the coating and the substrate, standards are not always available. The variability of thickness, layer composition, multilayer architectures, and substrate chemical nature creates difficulties in producing certified standards. This issue is critical in industrial applications; among them, determination of precious metal coatings in the fashion industry is certainly a major one, as production employs a large number of coatings and substrates, with extreme variability in the system to investigate.

Nowadays the most common approach is the use of the fundamental parameter (FP) method [6–9]. FP relies on a theoretical equation that considers the composition and thicknesses of the sample to evaluate the XRF intensity. Practically, the FP method is combined with few empirical standards to

© 2019 by the author(s). Distributed under a Creative Commons CC BY license.

Peer-reviewed version available at Coatings 2019, 9, 79; doi:10.3390/coatings9020079

correct unpredicted deviations eventually due to matrix effects[10,11]. With the FP method, it is possible to determine the film thickness of single and even multilayer samples if the structure and the composition are exactly known; nevertheless, the error correlated to the measurement is significant. Typical accuracy for single layer samples is ±5 %, while for multiple layer samples this value grows up to ±10 % for the upper layer and up to ±37 % for the first underlayer [2,12,13] due inaccuracy in the method for complex samples. Additionally, very often the thickness and composition of the underlying layers in multilayer architectures are not exactly known and introduced in the measurement software using and initial estimate [14].

The challenge of this work is to reduce this source of error in the results and their dependence on standards introducing a new semi-quantitative method (only the pure element spectra will need to be measured) based on Monte Carlo (MC) simulations. MC simulate X-ray spectra using a statistical approach that counts the photons interactions in the sample. With this approach, inhomogeneities of the sample, spectral and spatial distribution of the beam, polarisation effects, photo-absorption, multiple fluorescence, and scattering effects can be considered. Thickness gauging using the MC method is already reported in the literature; most of the reported works are in the field of cultural heritage applications [15–19]. In these cases, simulations are compared with the experimental measurement to confirm hypothesis based on bulk chemical composition, structural observations and historical information.

The approach described in this article differs from state of the art in the sense that we use simulations to build calibration curves to determine the thickness of the coating. The same calibration curve could be used for many samples instead of performing many simulations based on hypothesis. This concept will be particularly interesting for industrial applications in metal deposition factories. The simulations require a fast MC code, that is presently part of two software programs for such application: XRMC [20] and XMI-MSIM [21,22]. Both codes use the Xraylib database [23]. XRMC is generally used for complex 3D geometries since XMI-MSIM can only simulate samples composed of parallel layers. However, we decided to use XMI-MSIM because in our case the geometry is simple, and this program is currently superior to XRMC in simulating XRF experiments [20]. XMI-MSIM is the successor of MSIM, with a history of improvements of over 25 years [24–27].

In this work we examined a single layer sample of Au, Pd, Sn and white bronze on brass, using both certified single element coatings and electroplated alloys. The results were compared with other techniques for data validation: FP, FP + single empirical point and scanning electron microscopy equipped with a focused ion beam (FIB-SEM). This is expected to provide an analytical method to determine the thickness of coatings that does not make use of standards and whose performance is comparable or even better to those of XRF analysis with energy dispersive (ED-XRF) systems on metallic coatings. Finally, we varied some parameters in the simulation to find out the ones that are critical for the measurement and those that can be neglected to obtain reliable results.

2. Materials and Methods

The metal substrate consists of 3.75 x 5 mm brass (copper-zinc alloy) plates, 0.25 mm thick. The substrate was electroplated with palladium and gold using a commercial galvanic bath “720 PDFE MPM” and “8693 MUP” from Bluclad srl (Prato, Italy) and with white brass bath “SCUDO BIANCO PLUS RACK” from MacDermid (Waterbury, CT, USA). The alloy composition and layer thickness of the coatings are the subject of this study, and thus they will be discussed later. Certified samples with known thickness are also used and were provided by Bowman (Schaumburg, IL, USA).

XRF measurements were performed with the Bowman B Series XRF spectrometer using an acquisition time of 60 s, 50 kV tube voltage, 0.8 mA tube current and a collimator of 0.305 mm in diameter. The same spectra were used to obtain the thickness information with various methods: FP, FP with one empirical point correction (both available with the commercial software of the instrument) and the MC method proposed in this study.

The composition of the substrate and the coatings were measured with energy dispersive X-ray spectroscopy (EDS) microanalysis applying an accelerating voltage of 20 kV and scanning an area of approximately 0.1 mm^2 for a live time of 120 s. In order to consider the matrix effect, the ZAF

Preprints (www.preprints.org) | NOT PEER-REVIEWED | Posted: 24 January 2019 doi:10.20944/preprints201901.0244.v1

Peer-reviewed version available at *Coatings* **2019**, *9*, 79; doi:10.3390/coatings9020079

correction algorithm (atomic number, absorption and fluorescence) was used for quantification. For this purpose, a gold-plated, a palladium plated, and a white bronze plated sample were prepared, whose thicknesses were high enough to be considered infinite for the EDS analysis. The EDS analysis was performed with a Hitachi (Tokyo, Japan) S-2300 equipped with a Thermo Scientific (Waltham, MA, USA) Noran System 7 detector and analysed with Pathfinder software [28].

The SEM images and the FIB ablation were performed with a Tescan (Brno, Czech Republic) GAIA 3 equipped with the Triglav electron column and the Gallium FIB Cobra Gallium column

XRF spectra simulations were performed with the open source software XMI-MSIM v7.0 64-bit by Tom Schoonjans [21,22] which predicts the spectral response of ED-XRF using MC simulations. The software allows setting many variables of the system under investigation as well as the hardware geometry: this information was used as input to simulate the spectra.

The quantification method consisted of using the simulated spectra of 5 different layer thicknesses to build a calibration curve, which was used to extrapolate the unknown thicknesses of the measured samples. Simulations were performed using the exact composition of the coatings and the substrates that were measured with EDS. The spectrum of each pure element of interest (Cu, Zn, Pd, Sn and Au) was also both measured and simulated to obtain the relative intensity of the peak of interest, called Peak Ratio (PR) henceforth. The PR concept is similar to the K-ratio used in the EDS [29,30] and consists in the ratio between the peak intensity (X-ray counts) for the element of interest in the sample and the peak intensity at the same energy for the pure element (equation 1).

$$PR_i = \frac{I_i^{sample}}{I_i^{pure}} \tag{1}$$

XRF spectra were interpolated through multiple Gaussian [31–34] functions in the proximity of the energy lines of the expected elements to obtain the peak area. The considered peaks were Cu Kα, Zn Kα, Au Lα, Pd Kα and Sn Kα; in addition Cu Kβ and Zn Kβ were also fitted to avoid errors due to peak overlaps. The PR were calculated, and the resulting data were fitted with a second order curve. This kind of function is commonly implemented in XRF systems for industrial applications since it is in good agreement with experimental data for a limited range of thicknesses and it is moreover easy to manage. The complete quantification procedure is summarized in Figure 1.

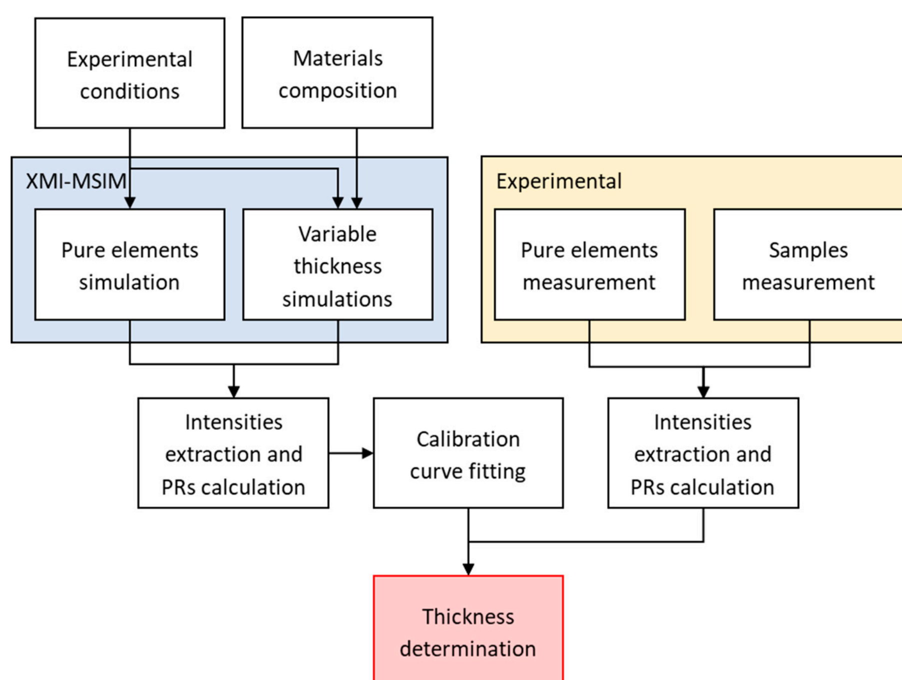

Figure 1. Flowchart of the algorithm used for the quantification process.

Preprints (www.preprints.org) | NOT PEER-REVIEWED | Posted: 24 January 2019 doi:10.20944/preprints201901.0244.v1

Peer-reviewed version available at *Coatings* **2019**, *9*, 79; doi:10.3390/coatings9020079

3. Results

3.1. Software Validation

The applicability of the proposed method is strongly connected to the ability of the simulation software to provide good results; for this reason, we evaluated the accuracy and the reproducibility of XMI-MSIM.

A parameter that affects the accuracy of the simulations is the number of interactions per trajectory: this number determines the maximum number of interactions that a photon can experience during its trajectory. Low values bring to truncation errors, but too high values could result in a computationally expensive simulation without any significant benefits in the results. Simulation of 1 μm of gold coating on brass was performed using values from 1 to 10 as the number of interactions; the PR of each element for all the spectra was compared to the simulation with the highest number of interactions permitted, and the relative deviation was calculated (Figure 2a). The results show an exponential improvement for the first 4 interactions then, by increasing the number of interactions, the deviation remains stable around 0.001 %: for this reason, all the following simulations were performed using 4 interactions per trajectory.

The precision of the simulated spectra was evaluated repeating the same simulation on samples consisting of 1 μm of gold on brass substrates 10 times. Then the deviation of the PR of each element from the mean value was calculated (Figure 2b) as well as the relative standard deviation, that results to be around 0.1 %.

After these tests, it can be concluded that the software results are good enough to allow its use in the study and to proceed with the following experiments.

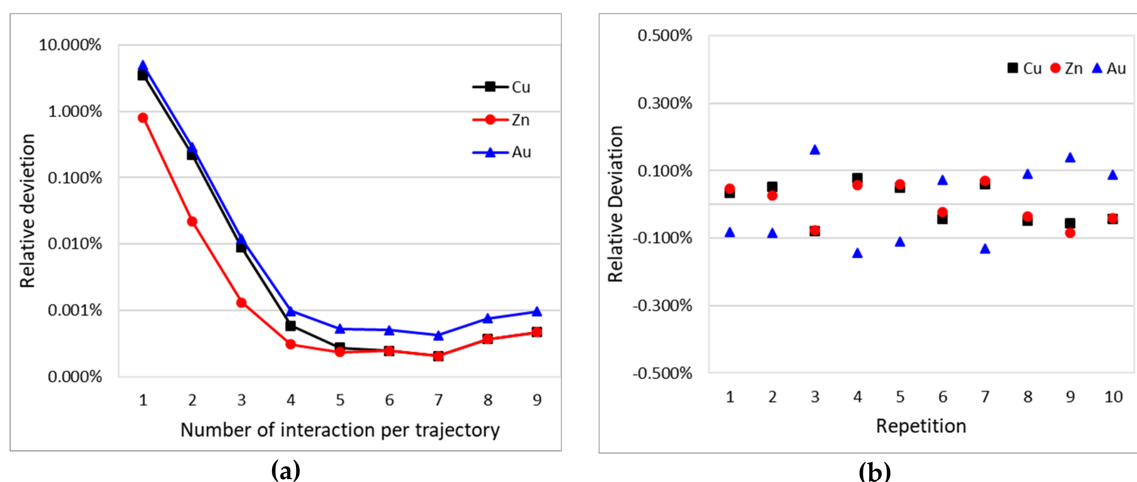

Figure 2. PRs of Cu, Zn and Au of a simulated 1 μm of gold coating on brass substrates. (a) Relative deviation of the PRs increasing the number of interactions respect to the simulation with 10 interactions; (b) relative deviation from the mean value repeating 10 times the same simulation.

3.2. Thickness Determination

After the preparation of the samples, they were measured with the XRF, then the spectra of certified samples and the pure elements Au and Pd were collected. The FP method considers the precious coating as pure for the thickness quantification. It was used both alone and combined with a single empirical point. For the empirical point, the certified calibration standards were used. Then, the thickness of the electroplated sample was measured with FIB-SEM performing a semi-destructive micro-cross-section (Figure 3).

Peer-reviewed version available at Coatings 2019, 9, 79; doi:10.3390/coatings9020079

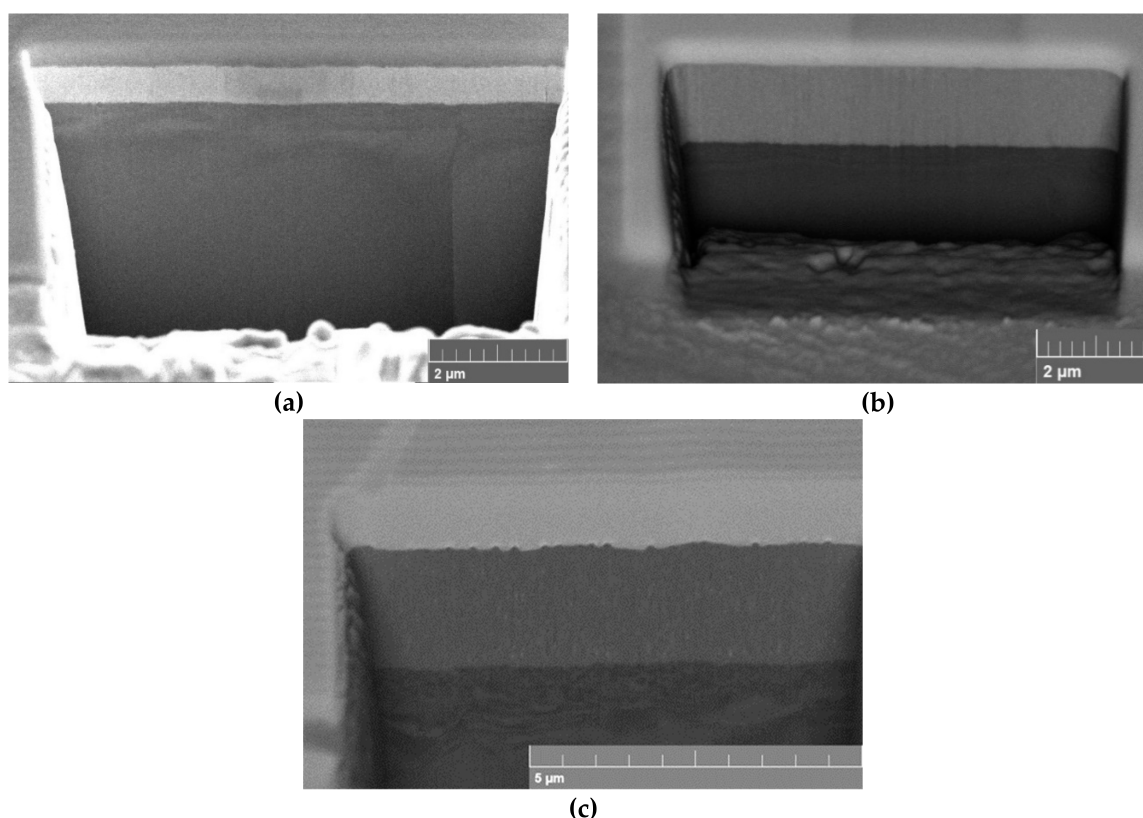

(a) (b) (c)

155 **Figure 3.** FIB-SEM images of the electroplated samples: (a) gold, (b) palladium and (c) white bronze.

156 A thick deposit of Au and Pd was electroplated separately (approximately 1.1 µm and 1.9 µm,
157 measured with XRF) and measured with EDS to find the actual composition (Table 1). The
158 composition of the certified thicknesses standards is known and is reported in Table 1 as well. The
159 results agree with the technical sheets of the baths; except the bronze that show a level of Sn higher
160 (47.2 %) than expected (28 – 35 %), this information will be useful in the determination of the
161 thickness.

162 **Table 1.** The composition of the substrate and the film investigated using EDS analysis.

Samples	Electroplated	Certified
Brass (substrate)	Cu: 63.0 wt% Zn: 37.0 wt%	Cu: 63.0 wt% Zn: 37.0 wt%
Au	Au: 97.9 wt% Fe: 1.6 wt% Ni: 0.5 wt%	Au: 100 wt%
Pd	Pd: 95.2 wt% Fe: 4.8 wt%	Pd: 100 wt%
Bronze / Sn	Cu: 39.9 wt% Zn: 12.9 wt% Sn: 47.2 wt%	Sn: 100 wt%

163 Besides that, we performed the simulations with XMI-MSIM using the exact concentrations;
164 moreover, the intensities of the peaks were integrated using a multiple Gaussian peak fit. The spectra
165 of the pure elements Au and Pd were also simulated to obtain the PRs. Finally, we obtained six
166 calibration curves (Figure 4), each one containing 5 points corresponding to different thickness values
167 of the metal: for electroplated gold, certified gold, electroplated palladium, certified palladium and
168 certified Sn we use 0.1, 0.5, 1.0, 1.5, and 2.0 µm thicknesses, while for electroplated white bronze we

Preprints (www.preprints.org) | NOT PEER-REVIEWED | Posted: 24 January 2019 doi:10.20944/preprints201901.0244.v1

Peer-reviewed version available at Coatings 2019, 9, 79; doi:10.3390/coatings9020079

use 0.1, 0.75, 1.5, 2.25 and 3 µm, since we expected a thicker coating. The points were fitted with a second order curve obtaining an $R^2 > 0.9999$.

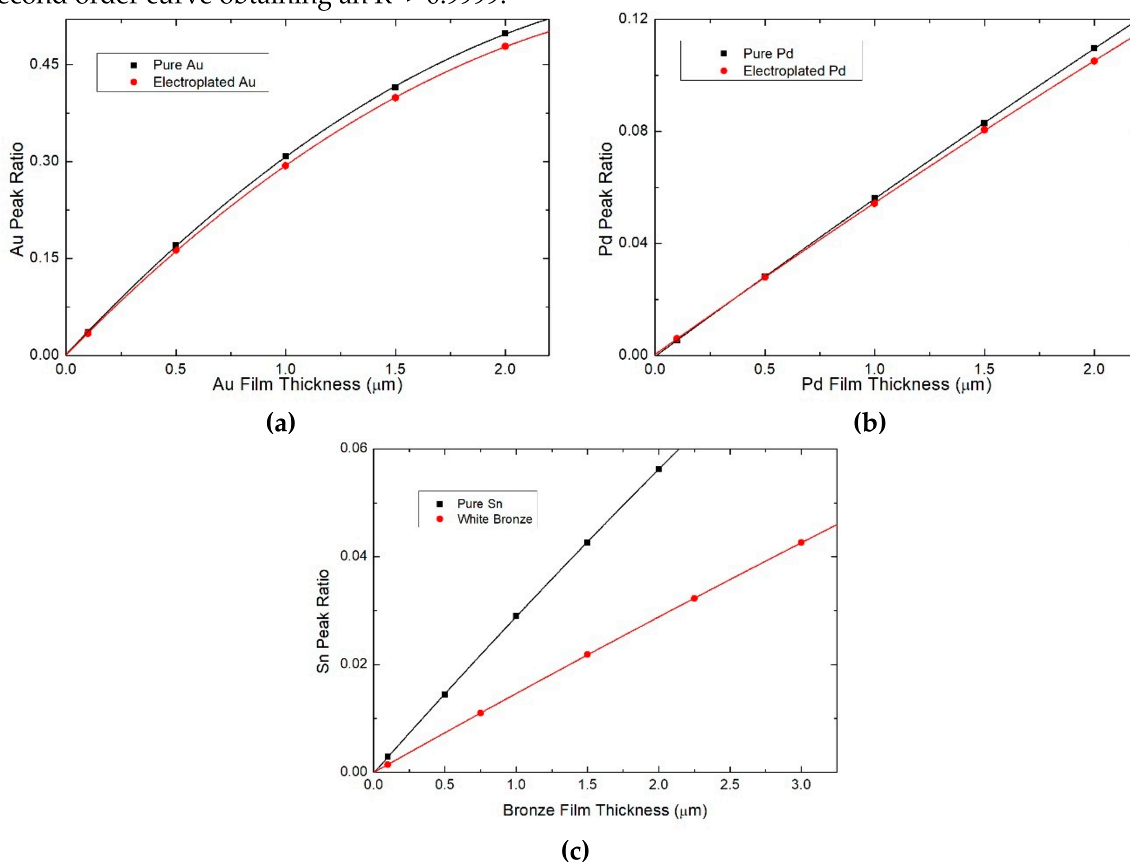

Figure 4. Calibration curves built from the simulations using the pure metals (black) and the composition of the electroplated films (red) of (a) Au, (b) Pd and (c) Sn.

The peak intensities in the measured spectra were fitted with the same multiple Gaussian curves to calculate PRs values and finding the thickness of the samples. The results (Table 2) show a big discrepancy in all the samples between the nominal value and the FP method; this deviation is highly improved with the empirical correction. Keeping in mind that the certified samples were also used as standards for the empirical correction, the good results obtained for the certified samples are not very surprising; besides that, the result in the case of the electroplated samples are improved but still with high accuracy error. On the other hand, the results obtained with the MC method are very promising: the estimated difference is below 2 % in four out of six cases, and for two samples the difference (0.0 %) is under the precision of the measurements. The case of electroplated palladium and bronze the deviation is higher, around 5 %, but they are still better than the FP result. The causes that produce these outliers will be studied in deep in the future, but we can advance hypotheses based on what we observed during the quantification process. The Sn and Pd peaks are not very intense, due to the characteristics of the samples and the detector, in these cases the signal to noise ratio not very high, for the same reason also the matrix effect and the background subtraction are important factors that must be taken in great consideration for accurate quantification.

The fitting of the calibration curve is good enough that if it is repeated by considering only 3 among the 5 simulated spectra, the variation will be only of approximately only ±0.3 %, meaning that, in the case, this variation could be acceptable, the computational cost could be decreased substantially. On the other hand, we found that the film composition influences the results strongly: in Figure 4 there is an appreciable divergence, increasing the thickness, using pure metal coating standards or the electrodeposited alloy, even if the composition varies only of few percental points. If the pure standards were used for the quantification of the galvanic sample, the results would have a variation of up to 5 %. About that we must mention that the result of FP for the electroplated bronze,

Preprints (www.preprints.org) | NOT PEER-REVIEWED | Posted: 24 January 2019 doi:10.20944/preprints201901.0244.v1

Peer-reviewed version available at Coatings 2019, 9, 79; doi:10.3390/coatings9020079

with the expected Sn concentration in the alloy was 35 %, it would have been 2.71 μm (54 % deviation from the real value), for this reason, we performed the EDS analysis to obtain the exact composition. Unfortunately, often it is assumed that the composition of the deposit does not change much over time, leading to gross errors.

Table 2. Nominal (Certified and FIB-SEM) and measured (XRF) thickness calculated with FP and MC methods for the samples.

Samples	Nominal	Experimental					
	Certification (μm)	FP (μm)	Difference (%)	FP + Empirical (μm)	Difference (%)	MC (μm)	Difference (%)
Certified Au	1.07	0.77	-28.0	1.07	0.0	1.08	+0.9
Certified Pd	1.02	0.82	-19.6	1.01	-1.0	1.02	0.0
Certified Sn	2.08	1.42	-31.7	2.01	-3.4	2.04	-1.9
	SEM (μm)						
Electroplated Au	0.53	0.28	-47.2	0.39	-26.4	0.53	0.0
Electroplated Pd	1.30	1.15	-11.5	1.40	+7.7	1.23	-5.4
Electroplated Bronze	1.76	1.31	-25.6	2.01	+14.2	1.85	+5.1

3.3. Critical parameters of measurement

In the previous section, we proved the power of the MC method for thickness determination. Then, more simulations were performed to predict the critical parameter that we need to take into account when we measure a sample, regardless of the measurement method used.

The first variable we considered was the thickness of the substrate: on too thin samples, the X-rays could pass through giving a PR different from those expected. To investigate this phenomenon, we simulated sandwich-like samples with 0.5 μm pure gold coating on both sides (to mimic a real galvanic sample) and a brass layer in between, whose thickness ranged from only 1 μm up to 1 cm, and we performed one simulation per order of magnitude. The influence of the thickness of brass substrates is evident only for very thin dimensions (Figure 5a): over 0.1 mm, the difference to an infinite bulk substrate is negligible, and the same calibration curve can be used for different samples.

Later, we investigated the influence of the alloy composition of both the coating and the substrate on the PR. We examined typical deposits of common thickness used in galvanic industry: 0.5 μm gold coating alloy, 3 μm white bronze alloy and brass alloys. The expected variation in the PR varying the composition of the alloys depends on secondary fluorescence and self-absorption of the sample, which depends on the composition, meaning that for different elements the trend could be different.

We investigated the influence of the brass composition on the Au PR. We simulated a 0.5 μm pure gold coating on 1 cm brass substrate. Typical brasses are alloys of Cu and Zn in ratios ranging from 62:38 (UNS alloy number C27200) to 70:30 (C26130) [35]. We simulated the following concentration of Cu: 63 %, 65 %, 67 % and 69 %. In this range of concentration, the Au PRs does not change significantly remaining in the error of the simulation (Figure 5b); the influence of the substrate could be more remarkable for higher differences in the composition [36].

Then, the effect of the alloy composition of the coating was studied. First, we investigated the Au-Cu alloy from pure gold to 18 kt (75 wt% Au) every 2 kt. As expected, the PR varies with the concentration but, as also found for the electroplated gold with pure gold calibration curve, the variation is bigger than the variation of gold concentration (Figure 5c); 22 kt gold (8.28 wt% Cu) gives a value of -16.1 % with respect to the 24 kt while 18 kt gold (25 wt% Cu) gives -41.0 %. These findings indicate that the results obtained with a not appropriated calibration curve cannot be corrected

Preprints (www.preprints.org) | NOT PEER-REVIEWED | Posted: 24 January 2019 doi:10.20944/preprints201901.0244.v1

Peer-reviewed version available at Coatings 2019, 9, 79; doi:10.3390/coatings9020079

231 simply using a multiplicative factor even if the composition is known. For example, if an 18 kt gold
232 sample is measured and the thickness is estimated with a 24 kt curve to be 0.5 μm, we cannot affirm
233 that the actual thickness is 0.5 μm*24 kt/18 kt = 0.67 μm since this would underestimate much the
234 value.
235 The same study was carried out with a white bronze alloy on brass. The typical galvanic white
236 bronze composition is 50 – 55 wt% Cu, 28 – 32 wt% Sn, 14 – 20 wt% Sn. The calibration curve is
237 typically built using a standard of pure Sn, and the results are multiplied by 3.33 (assuming a 30 wt%
238 of Sn in the alloy). We simulated an alloy keeping fixed the amount of Zn at 17 % and varying the
239 concentration of Cu and Sn, using Sn concentrations from 28 wt% to 32 wt% every 1%. The simulated
240 sample consists of a 3 μm bronze layer, a 5 μm Cu layer and 1 cm of brass substrate: these thicknesses
241 and layer combinations are typical of nickel-free electrodeposition for wearable accessories. Also in
242 this case, similar to what we found for different alloys of gold, the composition plays a crucial role in
243 the thickness determination (Figure 5d) and the approximation, in this case, results in even worse
244 agreement: a variation of just 4 percentage points leads to an error of 12.2 %.
245 We also simulated a sample with 32 wt% Sn but with 10 μm of the underlying Cu layer, to see if
246 there would be any variation, but the thickness of the layer below didn't seem to have any significant
247 influence.

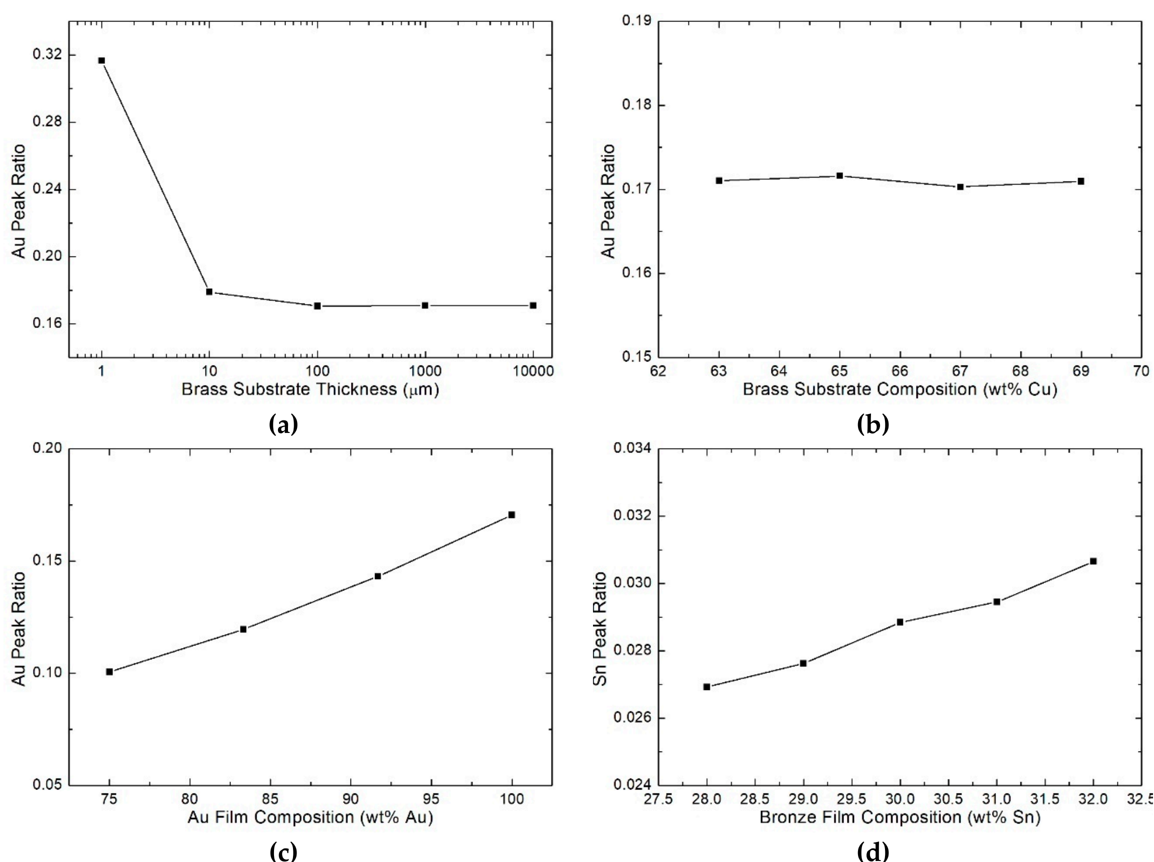

248 **Figure 5.** Dependence of Au PR, of 0.5 μm gold film on brass simulation, (a) on the thickness of the
249 substrate, (b) on the composition of the substrate (expressed in percentage of Cu) and (c) on the
250 composition of the film, increasing the amount of Cu. (d) Dependence of Sn PR, of 3 μm bronze film
251 on brass, on the composition of the film, increasing the amount of Cu.

252 ## 4. Conclusions

253 In the present work, we demonstrated the power of standardless MC calibration for measuring
254 the thickness of metallic coatings. We benchmarked the proposed method with the use of certified
255 standards and SEM imaging of FIB cross-sections. Our results indicate that the MC approach
256 competes well with the FP method that is the state of the art in the measurement of the thickness of

Preprints (www.preprints.org) | NOT PEER-REVIEWED | Posted: 24 January 2019 doi:10.20944/preprints201901.0244.v1

Peer-reviewed version available at *Coatings* **2019**, *9*, 79; doi:10.3390/coatings9020079

metallic coatings in industry. Remarkably, this result was achieved without the use of a standard of known thickness and composition.

The MC method has two major advantages: i) without the need of using standards allow an easy switch between materials and coating architectures and ii) it can easily adapt to existing XRF commercial systems as it requires only changes in the software.

After having validated the method and proved that the simulations give reliable results, we have explored a few critical situations that may lead to major errors in the measurement both with the FP and MC methods. We found that in the cases investigated, small variations in the composition and the thickness of the substrate, or other eventual layers in multilayer architectures, don't play a substantial role on the PR of the element on the top. Conversely, the composition of the substrate alloy must be exactly known; even a little deviation from the known composition can indeed bring to large errors in thickness quantification.

In this work we have used the MC method to investigate the thickness limited to a single layer on a substrate. In future, we will extend the technique to multilayer structures introducing a multivariable approach. Such investigation is currently in progress.

Funding: This research was funded by Regione Toscana POR CreO FESR 2014-2020 – azione 1.1.5 sub-azione a1 Bando 2 "Progetti di ricerca e sviluppo delle MPMI" which made possible the project "Gioielli in Argento Da Galvanica Ecologica e Tecnologica" (GADGET) and "Tecnologia al plasma per l'industria del lusso: una manifattura innovativa nel comparto accessori in ottica 4.0" (THIN FASHION).

Acknowledgments: In this section you can acknowledge any support given which is not covered by the author contribution or funding sections. This may include administrative and technical support, or donations in kind (e.g., materials used for experiments). Bowman Coating Measurements Systems is gratefully acknowledged for having provided technical information about the hardware and the internal geometry of the instrument. Authors acknowledge Mr. Carlo Bartoli for the support given in keeping the FIB-SEM up and running.

Authors contribution: W.G. performed XRF measurements, MC simulations, data analysis and interpretation and wrote the paper; E.B. performed part of the FIB SEM measurements; M.I. gave advice on the systems to be investigated, on the electrodeposition of the materials and on paper revising; A.L. conceived the work, supervised research, data analysis and paper writing.

Conflicts of Interest: The authors declare no conflict of interest.

References

1. Giurlani, W.; Zangari, G.; Gambinossi, F.; Passaponti, M.; Salvietti, E.; Di Benedetto, F.; Caporali, S.; Innocenti, M. Electroplating for Decorative Applications: Recent Trends in Research and Development. *Coatings* **2018**, *8*, 260, doi:10.3390/coatings8080260.
2. Nygård, K.; Hämäläinen, K.; Manninen, S.; Jalas, P.; Ruottinen, J. P. Quantitative thickness determination using x-ray fluorescence: Application to multiple layers. *X-Ray Spectrom.* **2004**, *33*, 354–359, doi:10.1002/xrs.729.
3. Fiorini, C.; Gianoncelli, A.; Longoni, A.; Zaraga, F. Determination of the thickness of coatings by means of a new XRF spectrometer. *Arch. Intern. Med.* **1992**, *152*, 1969–1971, doi:10.1002/xrs.550.
4. Jalas, P.; Ruottinen, J.; Hemminki, S. XRF Analysis of jewelry using fully standardless fundamental parameter approach. *Gold Technol.* **2002**, *35*, 28–34.
5. Sitko, R. Quantitative X-ray fluorescence analysis of samples of less than "infinite thickness": Difficulties and possibilities. *Spectrochim. Acta - Part B At. Spectrosc.* **2009**, *64*, 1161–1172, doi:10.1016/j.sab.2009.09.005.
6. Criss, J. W.; Birks, L. S. Calculation Methods for Fluorescent X-Ray Spectrometry: Empirical Coefficients vs. Fundamental Parameters. *Anal. Chem.* **1968**, *40*, 1080–1086, doi:10.1021/ac60263a023.
7. Kataoka, Y. Standardless x-ray fluorescence spectrometry (Fundamental Parameter Method using Sensitivity Library). *Rigaku J.* **1989**, *6*, 33–40.
8. Thomsen, V. Basic Fundamental Parameters in X-Ray Fluorescence. *Spectroscopy* **2007**, *22*, 46–50.
9. Takahara, H. Thickness and composition analysis of thin film samples using FP method by XRF analysis. *Rigaku J.* **2017**, *33*, 17–21.
10. Han, X. Y.; Zhuo, S. J.; Shen, R. X.; Wang, P. L.; Ji, A. Comparison of the quantitative results corrected by fundamental parameter method and difference calibration specimens in X-ray fluorescence spectrometry. *J. Quant. Spectrosc. Radiat. Transf.* **2006**, *97*, 68–74, doi:10.1016/j.jqsrt.2004.12.018.

Preprints (www.preprints.org) | NOT PEER-REVIEWED | Posted: 24 January 2019 doi:10.20944/preprints201901.0244.v1

Peer-reviewed version available at *Coatings* **2019**, *9*, 79; doi:10.3390/coatings9020079

309 11. Pessanha, S.; Fonseca, C.; Santos, J. P.; Carvalho, M. L.; Dias, A. A. Comparison of standard-based and
310 standardless methods of quantification used in X-ray fluorescence analysis: Application to the exoskeleton
311 of clams. *X-Ray Spectrom.* **2018**, *47*, 108–115, doi:10.1002/xrs.2819.
312 12. Vrielink, J. A. M.; Tiggelaar, R. M.; Gardeniers, J. G. E.; Lefferts, L. Applicability of X-ray fluorescence
313 spectroscopy as method to determine thickness and composition of stacks of metal thin films: A
314 comparison with imaging and profilometry. *Thin Solid Films* **2012**, *520*, 1740–1744,
315 doi:10.1016/j.tsf.2011.08.049.
316 13. Elam, W. T. T.; Shen, R. B.; Scruggs, B.; Nicolosi, J. Accuracy of Standardless FP Analysis of Bulk and Thin
317 Film Samples Using a New Atomic Database. *Adv. X-ray Anal.* **2004**, *47*, 104–109.
318 14. Ager, F. J.; Ferretti, M.; Grilli, M. L.; Juanes, D.; Ortega-Feliu, I.; Respaldiza, M. A.; Roldán, C.; Scrivano, S.
319 Reconsidering the accuracy of X-ray fluorescence and ion beam based methods when used to measure the
320 thickness of ancient gildings. *Spectrochim. Acta - Part B At. Spectrosc.* **2017**, *135*, 42–47,
321 doi:10.1016/j.sab.2017.06.017.
322 15. Schiavon, N.; de Palmas, A.; Bulla, C.; Piga, G.; Brunetti, A. An Energy-Dispersive X-Ray Fluorescence
323 Spectrometry and Monte Carlo simulation study of Iron-Age Nuragic small bronzes ("Navicelle") from
324 Sardinia, Italy. *Spectrochim. Acta - Part B At. Spectrosc.* **2016**, *123*, 42–46, doi:10.1016/j.sab.2016.07.011.
325 16. Bottaini, C. E.; Brunetti, A.; Montero-Ruiz, I.; Valera, A.; Candeias, A.; Mirão, J. Use of Monte Carlo
326 Simulation as a Tool for the Nondestructive Energy Dispersive X-ray Fluorescence (ED-XRF) Spectroscopy
327 Analysis of Archaeological Copper-Based Artifacts from the Chalcolithic Site of Perdigões, Southern
328 Portugal. *Appl. Spectrosc.* **2018**, *72*, 17–27, doi:10.1177/0003702817721934.
329 17. West, M.; Ellis, A. T.; Streli, C.; Vanhoof, C.; Wobrauschek, P. 2017 atomic spectrometry update-a review of
330 advances in X-ray fluorescence spectrometry and its special applications. *J. Anal. At. Spectrom.* **2017**, *32*,
331 1629–1649, doi:10.1039/c7ja90035j.
332 18. Brunetti, A.; Fabian, J.; La Torre, C. W.; Schiavon, N. A combined XRF/Monte Carlo simulation study of
333 multilayered Peruvian metal artifacts from the tomb of the Priestess of Chornancap. *Appl. Phys. A Mater.*
334 *Sci. Process.* **2016**, *122*, doi:10.1007/s00339-016-0096-6.
335 19. Barrea, R. A.; Bengió, S.; Derosa, P. A.; Mainardi, R. T. Absolute mass thickness determination of thin
336 samples by X-ray fluorescence analysis. *Nucl. Instruments Methods Phys. Res. Sect. B Beam Interact. with*
337 *Mater. Atoms* **1998**, *143*, 561–568, doi:10.1016/S0168-583X(98)00412-1.
338 20. Golosio, B.; Schoonjans, T.; Brunetti, A.; Oliva, P.; Masala, G. L. Monte Carlo simulation of X-ray imaging
339 and spectroscopy experiments using quadric geometry and variance reduction techniques. *Comput. Phys.*
340 *Commun.* **2014**, *185*, 1044–1052, doi:10.1016/j.cpc.2013.10.034.
341 21. Schoonjans, T.; Vincze, L.; Solé, V. A.; Sanchez Del Rio, M.; Brondeel, P.; Silversmit, G.; Appel, K.; Ferrero,
342 C. A general Monte Carlo simulation of energy dispersive X-ray fluorescence spectrometers - Part 5:
343 Polarized radiation, stratified samples, cascade effects, M-lines. *Spectrochim. Acta - Part B At. Spectrosc.* **2012**,
344 *70*, 10–23, doi:10.1016/j.sab.2012.03.011.
345 22. Schoonjans, T.; Solé, V. A.; Vincze, L.; Sanchez Del Rio, M.; Appel, K.; Ferrero, C. A general Monte Carlo
346 simulation of energy-dispersive X-ray fluorescence spectrometers - Part 6. Quantification through iterative
347 simulations. *Spectrochim. Acta - Part B At. Spectrosc.* **2013**, *82*, 36–41, doi:10.1016/j.sab.2012.12.011.
348 23. Schoonjans, T.; Brunetti, A.; Golosio, B.; Sanchez Del Rio, M.; Solé, V. A.; Ferrero, C.; Vincze, L. The xraylib
349 library for X-ray-matter interactions. Recent developments. *Spectrochim. Acta - Part B At. Spectrosc.* **2011**, *66*,
350 776–784, doi:10.1016/j.sab.2011.09.011.
351 24. Vincze, L.; Janssens, K.; Adams, F.; Jones, K. W. A general Monte Carlo simulation of energy-dispersive X-
352 ray fluorescence spectrometers-I. Unpolarized radiation, homogeneous samples. *Spectrochim. Acta Part B*
353 *At. Spectrosc.* **1993**, *48*, 553–573, doi:10.1016/0584-8547(93)80060-8.
354 25. Vincze, L.; Janssens, K.; Adams, F.; Rivers, M. L.; Jones, K. W. A general Monte Carlo simulation of ED-
355 XRF spectrometers. II: Polarized monochromatic radiation, homogeneous samples. *Spectrochim. Acta Part*
356 *B At. Spectrosc.* **1995**, *50*, 127–147, doi:10.1016/0584-8547(94)00124-E.
357 26. Vincze, L.; Janssens, K.; Adams, F.; Jones, K. W. A general Monte Carlo simulation of energy-dispersive X-
358 ray fluorescence spectrometers. Part 3. Polarized polychromatic radiation, homogeneous samples.
359 *Spectrochim. Acta Part B At. Spectrosc.* **1995**, *50*, 1481–1500, doi:10.1016/0584-8547(95)01361-X.
360 27. Vincze, L.; Janssens, K.; Vekemans, B.; Adams, F. Monte Carlo simulation of X-ray fluorescence spectra:
361 Part 4. Photon scattering at high X-ray energies. *Spectrochim. Acta Part B At. Spectrosc.* **1999**, *54*, 1711–1722,
362 doi:10.1016/S0584-8547(99)00094-4.

Preprints (www.preprints.org) | NOT PEER-REVIEWED | Posted: 24 January 2019 doi:10.20944/preprints201901.0244.v1

Peer-reviewed version available at *Coatings* **2019**, *9*, 79; doi:10.3390/coatings9020079

363 28. Pathfinder Available online: https://www.thermofisher.com/order/catalog/product/
364 IQLAADGABKFAQOMBJE (accessed on Dec 20, 2018).
365 29. Raymond Casting Application of Electron Probes to Local Chemical and Crystallographic Analysis, 1951.
366 30. Giurlani, W.; Innocenti, M.; Lavacchi, A. X-ray Microanalysis of Precious Metal Thin Films: Thickness and
367 Composition Determination. *Coatings* **2018**, *8*, 84, doi:10.3390/coatings8020084.
368 31. Watanabe, Y.; Kubozoe, T.; Mukoyama, T. Analytical functions for fitting K X-ray doublet peaks from Si(Li)
369 detectors. *Nucl. Inst. Methods Phys. Res. B* **1986**, *17*, 81–85, doi:10.1016/0168-583X(86)90456-8.
370 32. McNelles, L. A.; Campbell, J. L. Analytic approximations to peak shapes produced by Ge(Li) and Si(Li)
371 spectrometers. *Nucl. Instruments Methods* **1975**, *127*, 73–81, doi:10.1016/0029-554X(75)90304-3.
372 33. Van Espen, P.; Lemberge, P. Ed-Xrf Spectrum Evaluation and Quantitative Analysis Using Multivariate
373 and Nonlinear Techniques. *Adv. X-ray Anal.* **2000**, *43*, 560–569.
374 34. Kikongi, P.; Salvas, J.; Gosselin, R. Curve-fitting regression: improving light element quantification with
375 XRF. *X-Ray Spectrom.* **2017**, *46*, 347–355, doi:10.1002/xrs.2760.
376 35. Oberg, E.; Jones, F.; Horton, H.; Ryffel, H.; McCauley, C. *Machinery's Handbook*; 30th ed.; 2016; ISBN
377 9780831130923.
378 36. Fan, Q. Simulation of relationships between substrate XRF intensities and film thicknesses. *X-Ray Spectrom.*
379 **1993**, *22*, 11–12, doi:10.1002/xrs.1300220104.